

Received:  
10 January 2014

Revised:  
8 May 2014

Accepted:  
14 May 2014

doi: 10.1259/bjr.20140051

Cite this article as:

Ono A, Okada F, Takata S, Hiramatsu K, Ando Y, Nakayama T, et al. A comparative study of thin-section CT findings between seasonal influenza virus pneumonia and *Streptococcus pneumoniae* pneumonia. Br J Radiol 2014;87:20140051.

## FULL PAPER

# A comparative study of thin-section CT findings between seasonal influenza virus pneumonia and *Streptococcus pneumoniae* pneumonia

<sup>1</sup>A ONO, MD, <sup>1</sup>F OKADA, MD, <sup>2</sup>S TAKATA, MD, <sup>3</sup>K HIRAMATSU, MD, <sup>4</sup>Y ANDO, MD, <sup>2</sup>T NAKAYAMA, MD, <sup>5</sup>T MAEDA, MD and <sup>1</sup>H MORI, MD

<sup>1</sup>Department of Radiology, Oita University Faculty of Medicine, Oita, Japan

<sup>2</sup>Department of Radiology, Oita Red Cross Hospital, Oita, Japan

<sup>3</sup>Hospital Infection Control Center, Oita University Hospital, Oita, Japan

<sup>4</sup>Department of Radiology, Nishi Beppu National Hospital, Oita, Japan

<sup>5</sup>Department of Radiology, Oita Prefectural Hospital, Oita, Japan

Address correspondence to: Dr Asami Ono

E-mail: [asami@oita-u.ac.jp](mailto:asami@oita-u.ac.jp)

**Objective:** To compare the pulmonary thin-section CT findings in patients with seasonal influenza virus pneumonia with *Streptococcus pneumoniae* pneumonia.

**Methods:** The study group included 30 patients (20 males and 10 females; age range, 20–91 years; mean age, 55.9 years) with seasonal influenza virus pneumonia and 71 patients (47 males and 24 females; age range, 27–92 years; mean age, 67.5 years) with *S. pneumoniae* pneumonia.

**Results:** The proportion of community-acquired infection was significantly higher in patients with influenza virus pneumonia than with *S. pneumoniae* pneumonia ( $p = 0.001$ ). CT findings of ground-glass attenuation (GGA) ( $p = 0.012$ ) and crazy-paving appearance ( $p = 0.03$ ) were significantly more frequent in patients with influenza virus pneumonia than with *S. pneumoniae* pneumonia. Conversely, consolidation ( $p < 0.001$ ), mucoid impaction ( $p < 0.001$ ),

centrilobular nodules ( $p = 0.04$ ) and pleural effusion ( $p = 0.003$ ) were significantly more frequent in patients with *S. pneumoniae* pneumonia than in those with influenza virus pneumonia.

**Conclusion:** Pulmonary thin-section CT findings, such as consolidation and mucoid impaction may be useful in distinguishing between seasonal influenza virus pneumonia and *S. pneumoniae* pneumonia.

**Advances in knowledge:** (1) Distinguishing seasonal influenza virus pneumonia with *S. pneumoniae* pneumonia is important. (2) The CT findings of GGA and crazy-paving appearance were more frequently found in patients with influenza virus pneumonia than in patients with *S. pneumoniae* pneumonia, whereas consolidation, mucoid impaction, centrilobular nodules and pleural effusion were more frequently found in patients with *S. pneumoniae* pneumonia.

Influenza virus is responsible for seasonal epidemics of community-acquired pneumonia (CAP), with outbreaks occurring predominantly during the winter months. Secondary bacterial superinfections are the most frequent complications among fatal cases of seasonal and pandemic influenza.

*Streptococcus pneumoniae* is the most common pathogen of CAP and is also responsible for the increasing frequency of nosocomial pneumonia.<sup>1–3</sup> The mortality related with pneumonia is affected by initial antibiotic therapy; therefore, early detection of *S. pneumoniae* pneumonia is important for reducing mortality. Moreover, *S. pneumoniae* has been identified as the most prominent causative agent for secondary bacterial pneumonia following influenza virus infection.<sup>4</sup>

A rapid immunochromatographic membrane test was developed for the detection of *S. pneumoniae* antigens.<sup>5</sup> It is a useful technique for the rapid diagnosis of *S. pneumoniae* pneumonia; however, it does have its limitations. For example, urinary antigens of *S. pneumoniae* pneumonia cannot be detected a few days after *S. pneumoniae* infection, and assay sensitivity is approximately 70–80%.

There are several reports of the radiologic features of novel influenza virus pneumonia and *S. pneumoniae* pneumonia.<sup>6–8</sup> However, there are few reports of the CT findings of seasonal influenza virus pneumonia.<sup>9–11</sup> Furthermore, to the best of our knowledge, no studies comparing CT findings in patients with seasonal influenza virus pneumonia to those with *S. pneumoniae* pneumonia have been published. The present

study therefore compared the pulmonary thin-section CT findings of patients with seasonal influenza virus pneumonia to those with *S. pneumoniae* pneumonia.

## METHODS AND MATERIALS

### Patient population

This study was approved by the institutional review board and, because of its retrospective nature, informed consent was not required.

Based on the patient population of our institutions for the period January 2007 to September 2012, we retrospectively identified 482 consecutive adult patients with seasonal influenza virus infections and 276 consecutive adult patients with *S. pneumoniae* pneumonia.

Of the 482 patients with influenza virus infections, 393 were infected with influenza Type A virus (A) and 89 with Type B (B). Of these patients, 31 (A, 29 patients and B, 2 patients) were diagnosed with influenza virus pneumonia, and thin-section CT examinations of the chest were performed. A single patient diagnosed with concurrent *S. pneumoniae* pneumonia, as determined from serological tests and clinical findings, was excluded from the present study.

Serological tests and clinical findings determined that of the 276 patients with acute *S. pneumoniae* pneumonia, 90 were diagnosed with concurrent infectious diseases (42 with *Haemophilus influenzae*, 37 with *Staphylococcus aureus*, 18 with *Moraxella catarrhalis*, 18 with *Pseudomonas aeruginosa*, eight with *Klebsiella pneumoniae* and one with influenza virus) and were therefore excluded from the study. Of the remaining 186 patients solely infected with *S. pneumoniae*, 73 underwent thin-section CT examinations of the chest. Two patients with *S. pneumoniae* pneumonia were excluded from the study because of poor image quality of the CT scans; a result of motion artefacts.

The final study group included 30 patients with influenza virus (A, 28 patients and B, 2 patients) pneumonia (20 males and 10 females; age range, 20–91 years; mean age, 55.9 years), and 71 patients with *S. pneumoniae* pneumonia (47 males and 24 females; age range, 27–92 years; mean age, 67.5 years). Among the 71 patients, two patients with *S. pneumoniae* pneumonia after influenza virus infection were included.

A diagnosis of pneumonia was made when clinical syndromes, cough with or without sputum, fever, leucocytosis or leucopenia, and pulmonary infiltrates on the chest radiograph were present, and the symptoms coincided with the detection of influenza virus using an immunochromatography rapid diagnostic kit ( $n = 30$ ), or of *S. pneumoniae* isolated from sputum ( $n = 47$ ), tracheal aspirate ( $n = 15$ ), or both sputum and urine ( $n = 9$ ).

A patient was considered to have CAP if, at the time of hospital admission, he/she presented with respiratory symptoms and sputum, and exhibited pulmonary infiltrates on chest radiographs. No patient in our study had been admitted to or treated in a hospital in the 2 weeks prior to admission.

### CT examinations

Thin-section CT examinations were performed volumetrically with 8-, 31- or 64-detector CT system with a 1-mm reconstruction. CT was done during a breath hold at full inspiration with the patient in a supine position and was reconstructed using a high-spatial-frequency algorithm. Images were captured at window settings that allowed viewing of the lung parenchyma (window level,  $-600$  to  $-700$  HU; window width, 1200–1500 HU) and the mediastinum (window level, 20–40 HU; window width, 400 HU).

A pulmonary CT examination was performed within 1–7 days (mean, 1.1 days in patients with influenza virus pneumonia and 4 days in patients with *S. pneumoniae* pneumonia) after the onset of respiratory symptoms.

### Image interpretation

Two radiologists (with 25 and 11 years' experience in chest CT image interpretation) unaware of the underlying diagnoses, independently interpreted the CT images in random order. The final decision was reached by consensus.

CT images were assessed for the following radiological features: ground-glass attenuation (GGA), bronchial wall thickening, crazy-paving appearance, centrilobular nodules, interlobular septal thickening, consolidation, cavities, mucoid impaction, pleural effusion and enlarged hilar/mediastinal lymph node(s) ( $>1$ -cm diameter short axis). GGA was defined as an area showing hazy increases in attenuation without obscuring vascular markings.<sup>12,13</sup> Crazy-paving appearance was considered to be a network of a smooth linear pattern superimposed on an area of GGA.<sup>12,13</sup> Centrilobular nodules were defined as nodules around the peripheral pulmonary arterial branches or 3–5 mm from the pleura, interlobular septa or pulmonary veins. Interlobular septal thickening was defined as abnormal widening of the interlobular septa.<sup>13</sup> Consolidation was defined as an area of increased attenuation that obscured vascular markings.<sup>12,13</sup>

The distribution of parenchymal disease was also evaluated. We assessed whether the abnormal findings were located unilaterally or bilaterally. If the main lesion was predominantly located in the inner third of the lung, the disease was classified as a central distribution, whereas if the lesion was predominantly located in the outer third of the lung, the disease was classified as a peripheral distribution. If the lesions showed no predominant distribution, the disease was classified as randomly distributed. In addition, zonal predominance was classified as upper, lower or random. Upper lung zone predominance indicated that most abnormalities were seen at a level above the tracheal carina, whereas lower zone predominance indicated that most abnormalities were located below the upper zone. When abnormalities showed no clear zonal predominance, the lung disease was classified as randomly distributed.

### Statistical analysis

Statistical analysis for the frequency of symptoms and CT findings was conducted using the Fisher's exact test and  $\chi^2$  tests. A mean age comparison was conducted using Student's *t*-test.

Table 1. Characteristics of 101 patients with each type of pneumonia

| Characteristics    | Influenza virus<br>( <i>n</i> = 30) | <i>Streptococcus pneumoniae</i><br>( <i>n</i> = 71) |
|--------------------|-------------------------------------|---|
| Male/female        | 20/10                               | 47/24   |
| Age (years)        |                                     |   |
| Range              | 20–91                               | 27–92   |
| Mean               | 55.9                                | 67.5  |
| Community acquired | 30.0 (100.0)                        | 51.0 (71.8)   |
| Nosocomial         | 0.0 (0.0)                           | 20.0 (28.2)   |

Data in parentheses are percentages.

## RESULTS

### Patient profiles

The characteristics of all patients are summarized in Table 1. The mean age of patients with influenza virus pneumonia was lower than that of patients with *S. pneumoniae* pneumonia (Table 1). All 30 patients with influenza virus pneumonia had community-acquired infections. Of the 71 patients with *S. pneumoniae* pneumonia, 51 had community-acquired infections and 20 nosocomial infections. The proportion of community-acquired infection was significantly higher for patients with influenza virus pneumonia than those with *S. pneumoniae* pneumonia ( $p = 0.001$ ).

### CT patterns

The thoracic CT findings of the 101 patients are summarized in Table 2. For the 30 patients with influenza virus pneumonia, GGA ( $n = 30$ , 100%) and bronchial wall thickening ( $n = 14$ , 46.7%) were most frequent, followed by crazy-paving appearance ( $n = 8$ , 26.7%), centrilobular nodules ( $n = 7$ , 23.3%) and interlobular septal thickening ( $n = 3$ , 10.0%) (Figures 1 and 2). Cavity or mucoid impaction was not observed in any patient.

For the 71 patients with *S. pneumoniae* pneumonia, GGA ( $n = 58$ , 81.7%) was most frequent, followed by consolidation

( $n = 54$ , 76.1%), mucoid impaction ( $n = 37$ , 52.1%), centrilobular nodules ( $n = 32$ , 45.1%) and bronchial wall thickening ( $n = 30$ , 42.2%) (Figures 3–5). Crazy-paving appearance ( $n = 7$ , 9.9%) and interlobular septal thickening ( $n = 3$ , 4.2%) were also observed (Figure 3). No cavitory lesions were detected for any patient.

The frequencies of GGA and crazy-paving appearance were significantly higher in patients with influenza virus pneumonia compared with *S. pneumoniae* pneumonia ( $p = 0.012$  and  $p = 0.03$ , respectively) (Figures 1 and 2). Conversely, the frequencies of consolidation, mucoid impaction and centrilobular nodules were significantly higher in patients with *S. pneumoniae* pneumonia than in patients with influenza virus pneumonia ( $p < 0.001$ ,  $p < 0.001$ ,  $p = 0.04$ , respectively) (Figures 3–5). There were no significant differences for the other CT findings, including bronchial wall thickening and interlobular septal thickening, between the two groups.

### Disease distribution

In the influenza virus pneumonia group, abnormal findings were found unilaterally in 17 patients (56.7%) and bilaterally in 13 patients (43.3%). The predominant zonal distribution was the upper zone in 16 patients (53.3%) (Figure 1) and lower zone in 10 patients (33.3%) (Figure 2). In the *S. pneumoniae* pneumonia group, abnormal findings were found unilaterally in 31 patients (43.7%) and bilaterally in 40 patients (56.3%). The predominant zonal distribution was the upper zone in 26 patients (36.6%) (Figure 3) and lower zone in 29 patients (40.8%) (Figures 4 and 5). There were no significant differences in zonal distributions between the two groups.

For the group with influenza virus pneumonia, parenchymal abnormalities were observed to be predominantly randomly distributed ( $n = 16$ , 53.3%), and peripherally distributed in 14 patients (46.7%). For the group with *S. pneumoniae* pneumonia, parenchymal abnormalities were observed to be peripherally distributed ( $n = 50$ , 70.4%), and randomly distributed in 15 (21.1%) patients. The frequency of peripheral distribution was

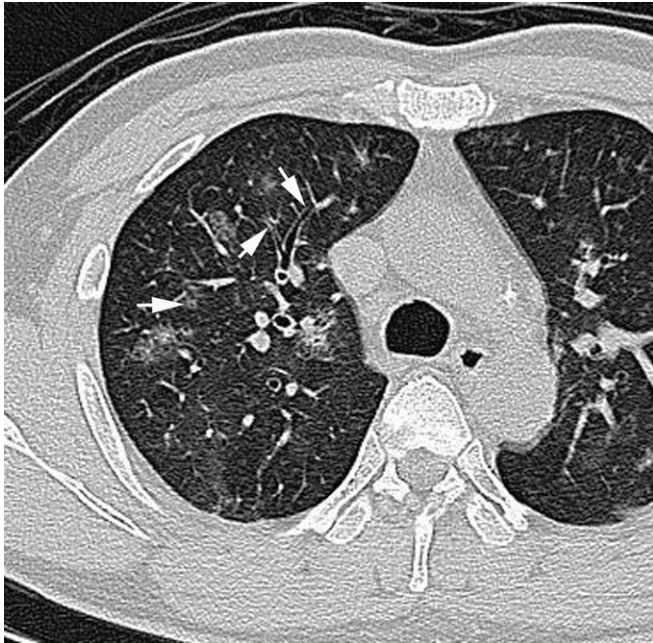
Table 2. Thoracic CT findings for each type of pneumonia

| Findings                       | Influenza virus ( <i>n</i> = 30) | <i>Streptococcus pneumoniae</i> ( <i>n</i> = 71) | <i>p</i> -value |
|--------------------------------|----------------------------------|--|-----------------|
| Ground-glass attenuation       | 30 (100.0)                       | 58 (81.7)  | 0.012           |
| Bronchial wall thickening      | 14 (46.7)                        | 30 (42.2)  | NS              |
| Crazy-paving appearance        | 8 (26.7)                         | 7 (9.9)  | 0.030           |
| Centrilobular nodules          | 7 (23.3)                         | 32 (45.1)  | 0.040           |
| Interlobular septal thickening | 3 (10.0)                         | 3 (4.2)  | NS              |
| Consolidation                  | 0 (0.0)                          | 54 (76.1)  | <0.001          |
| Cavity                         | 0 (0.0)                          | 0 (0.0)  | NS              |
| Mucoid impaction               | 0 (0.0)                          | 37 (52.1)  | <0.001          |
| Pleural effusion               | 0 (0.0)                          | 17 (23.9)  | 0.003           |
| Lymph node enlargement         | 0 (0.0)                          | 4 (5.6)  | NS              |

NS, not significant.

Data in parentheses are percentages.

Figure 1. Pneumonia caused by seasonal influenza virus (Type A) in a 41-year-old male, 1 day after the onset of cough and fever. Transverse CT image (1-mm thickness) of the right upper lobe shows ground-glass attenuation and bronchial wall thickening (arrows).



significantly higher in the *S. pneumoniae* pneumonia group than in the influenza virus pneumonia group ( $p = 0.024$ ).

#### Effusion and lymph nodes

Pleural effusion was found in 17 of the 71 patients with *S. pneumoniae* pneumonia (23.9%), and bilaterally in 11 patients (15.5%). The frequency of pleural effusion was significantly higher in patients with *S. pneumoniae* pneumonia than in those with influenza virus pneumonia ( $p = 0.003$ ).

Mediastinal and/or hilar lymph node enlargement was observed in four patients (5.6%) with *S. pneumoniae* pneumonia but was not observed for patients with influenza virus pneumonia. There was no significant difference between the two groups.

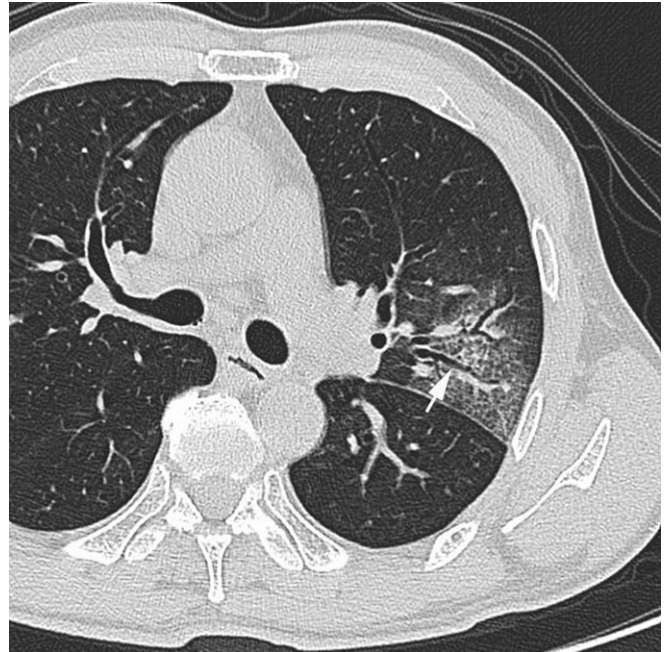
#### Follow-up study

All 30 patients with influenza virus pneumonia underwent antiviral therapy. All 71 patients with *S. pneumoniae* pneumonia underwent antibiotic therapy. For three of the patients with influenza virus pneumonia, a follow-up CT examination and/or chest radiography was performed, and abnormal findings showed improvement. For the remaining 27 patients with influenza virus pneumonia, their clinical symptoms had improved. For 64 (90%) patients with *S. pneumoniae* pneumonia, a follow-up CT examination and/or chest radiography demonstrated an improvement in abnormal findings. No deaths were reported for patients in either of the groups.

## DISCUSSION

Seasonal influenza virus is one of the most pandemic infections globally. Although influenza virus frequently causes severe

Figure 2. Pneumonia caused by influenza virus (Type A) in a 59-year-old male, 1 day after the onset of cough and fever. Transverse CT image (1-mm thickness) of the level of the left B3 division shows ground-glass attenuation, crazy-paving appearance and bronchial wall thickening (arrow).

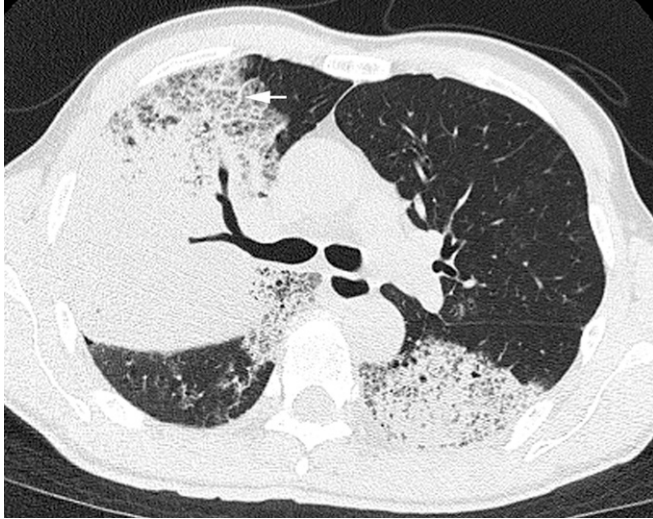


pneumonia, which can rapidly progress to acute respiratory distress syndrome, the greatest contributor to mortality is secondary bacterial infections.<sup>14–16</sup> The majority of patients who develop pneumonia are older and have severe comorbid conditions, such as heart disease, chronic obstructive pulmonary disease, renal disease, diabetes and immunosuppression. However, serious influenza virus pneumonia has also occurred in previously healthy patients.

There is strong and consistent evidence of epidemiological and clinically important interactions between influenza virus and secondary bacterial respiratory pathogens, particularly *S. pneumoniae*. Influenza virus infection causes the destruction of respiratory epithelium and virus neuramidase activity, which increases bacterial adhesion to epithelium.<sup>17</sup> Moreover, influenza virus infection leads to the synthesis of virus-activating bacterial proteases, and the inflammatory responses to viral infection may upregulate expression of molecules utilized as receptors by bacteria.<sup>17,18</sup> Seki et al<sup>19</sup> reported that “immune mediators, including cytokines and chemokines, through Toll-like receptor/mitogen-activated protein kinase pathways, play important roles in the pathology of co-infection caused by influenza virus and *S. pneumoniae*”. Another proposed mechanism, which pre-disposes the host to *S. pneumoniae* pneumonia, is influenza-induced Type 1 interferon sensitization to secondary bacterial infection.<sup>20</sup> Influenza virus infection also decreases tracheal mucociliary velocity and initial *S. pneumoniae* clearance, which results in an increase in *S. pneumoniae* burden.<sup>21</sup>

Autopsy findings have widely demonstrated that *S. pneumoniae* was the most common bacterial pathogen (29–48%) responsible

Figure 3. Pneumonia caused by *Streptococcus pneumoniae* in a 61-year-old male, 4 days after the onset of fever, cough with sputum and dyspnoea. Transverse CT image (1-mm thickness) at the level of the tracheal carina shows consolidation, ground-glass attenuation and crazy-paving appearance. Interlobular septal thickening is also present (arrow).



for superimposed infections in patients with influenza pneumonia, followed by *Staphylococcus aureus* (7–40%).<sup>22–26</sup>

A number of studies have reported on the radiological findings in *S. pneumoniae* pneumonia.<sup>6–8</sup> In the present study, our results

Figure 4. Pneumonia caused by *Streptococcus pneumoniae* in a 68-year-old male, 5 days after the onset of cough with sputum and fever. Transverse CT image (1-mm thickness) of the left lower lobe shows consolidation, ground-glass attenuation, centrilobular nodules (arrowheads) and mucoid impaction (arrows).

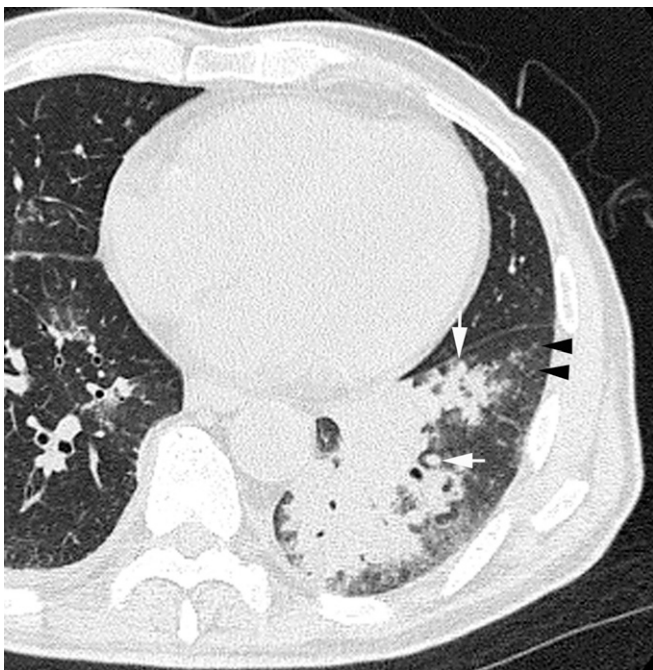
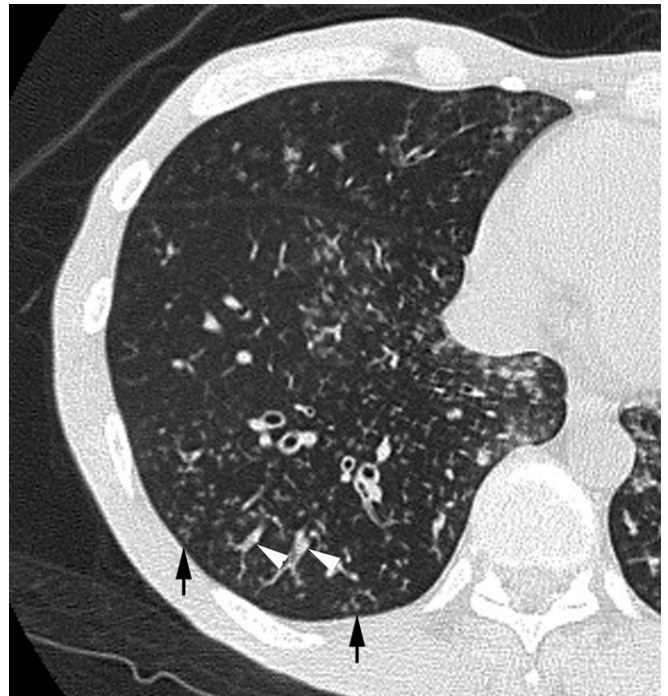


Figure 5. Pneumonia caused by *Streptococcus pneumoniae* in a 52-year-old male, 3 days after the onset of cough with sputum and fever. Transverse CT image (1-mm thickness) of right lower lobe shows bronchial wall thickening, mucoid impaction (arrowheads) and centrilobular nodules (arrows).



demonstrated that CT findings in patients with *S. pneumoniae* pneumonia consisted mainly of GGA, consolidation, mucoid impaction, centrilobular nodules and bronchial wall thickening. With the exception of frequency of mucoid impaction (no published data are available), our results were consistent with those reported elsewhere.<sup>6–8</sup>

A number of studies on radiologic findings in patients with novel influenza virus pneumonia were reported. However, there have been few studies conducted on the radiologic findings of seasonal influenza virus pneumonia;<sup>9–11,27,28</sup> furthermore, no reports have focused on the differences between seasonal influenza virus pneumonia and *S. pneumoniae* pneumonia.

With regard to the radiological findings in seasonal influenza virus pneumonia, Oikonomou et al<sup>9</sup> reported CT findings for four patients with haematologic malignancies. The CT findings from that study consisted of GGA, patchy consolidation, centrilobular nodules and branching linear opacities. Leung et al<sup>27</sup> reported on a single case of influenza virus B pneumonia from 59 cases of pulmonary infection in bone marrow transplant recipients. The chest radiograph showed multiple nodules in the middle and lower zones of both lungs. Information of the radiographic findings of seasonal influenza virus pneumonia in immunocompetent patients is also limited. Kim et al<sup>10</sup> evaluated CT findings in two patients and reported that both lungs had areas of multifocal peribronchovascular or subpleural consolidation with GGA. Recently, Tanaka et al<sup>11</sup> compared CT findings in 10 patients with seasonal influenza virus pneumonia with 19 patients with novel influenza virus pneumonia. They found that consolidation was more frequent

in novel influenza virus pneumonia and that reticular opacity occurred more frequently in seasonal influenza virus pneumonia. CT findings such as consolidation or lymph node enlargement were more frequently observed in their study, compared with what was observed in ours. Such discrepancies may have arisen because of the differences in the interval following the onset of respiratory symptoms and CT examinations or the differences in the pathological phases of diffuse alveolar damage or severities.<sup>29</sup> Further studies are needed to clarify the frequencies of the CT findings and using a larger sampling population.

In the present study, we compared the CT findings of seasonal influenza virus pneumonia with that of *S. pneumoniae* pneumonia. We found that the frequencies of GGA and crazy-paving appearance were significantly higher in patients with influenza virus pneumonia compared with *S. pneumoniae* pneumonia, whereas the frequencies of consolidation, mucoid impaction, centrilobular nodules and pleural effusion were significantly higher in patients with *S. pneumoniae* pneumonia.

Fujita et al<sup>28</sup> reported that on chest CT findings of 12 patients with influenza virus pneumonia, consolidation could not be observed from 7 patients with pure influenza virus pneumonia but could be observed from 5 patients with concurrent bacterial pneumonia. The results were consistent with those found in the present study.

In the pathological findings of influenza virus pneumonia, bronchial and bronchiolar walls are congested, mononuclear cells infiltrate the lumina and parenchymal changes exhibit typical features of diffuse alveolar damage.<sup>30,31</sup> It has also been reported that GGA and crazy-paving appearance correlated well with the pathological findings of diffuse alveolar

damage.<sup>29,32</sup> Therefore, the CT findings of GGA and crazy-paving appearance would be considerably more frequent in patients with influenza virus pneumonia than in *S. pneumoniae* pneumonia.

Conversely, *S. pneumoniae* pneumonia takes the form of lobar pneumonia, whereby alveolar lumens are filled with exudates containing leukocytes and alveolar walls are thickened by capillary congestion and oedema.<sup>33,34</sup> Therefore, CT findings, such as consolidation or mucoid impaction, in patients with *S. pneumoniae* pneumonia would be more frequently found than for influenza virus pneumonia.

It should be noted that there are several limitations to this study. First, this was a retrospective study and CT image interpretation was performed by consensus. Second, this study included only a small number of patients; therefore, it might be difficult to generalize the thin-section CT findings observed in this study as "characteristic findings". Third, no correlation with pathological findings was possible. Fourth, the thin-section CT images were obtained at several institutions using different protocols. Finally, CT images in the patients with both influenza virus and *S. pneumoniae* could not be evaluated because there was only one patient available in our institution.

In summary, the CT findings of GGA and crazy-paving appearance were more frequently found in patients with influenza virus pneumonia than for patients with *S. pneumoniae* pneumonia, while consolidation, mucoid impaction, centrilobular nodules and pleural effusion were more frequently found in patients with *S. pneumoniae* pneumonia. Consolidation and mucoid impaction were the most important findings, especially for discriminating between these two types of pneumonia.

## REFERENCES

- Craven DE, Steger KA. Epidemiology of nosocomial pneumonia. New perspective on an old disease. *Chest* 1995; **108**(2 Suppl): 1S–16S.
- Chastre J, Fagon JF. Pneumonia in the ventilator-dependent patient. In: Tobin M, ed. *Principles and practice of mechanical ventilation*. 1st edn. New York, NY: McGraw & Hill; 1994. pp. 857–90.
- American Thoracic Society. Hospital-acquired pneumonia in adults: diagnosis, assessment of severity, initial antimicrobial therapy, and preventive strategies: a consensus statement. *Am J Respir Crit Care Med* 1996; **153**: 1711–25.
- Lei TH, Hsia SH, Wu CT, Lin JJ. *Streptococcus pneumoniae*-associated haemolytic uremic syndrome following influenza A virus infection. *Eur J Pediatr* 2010; **169**: 237–9. doi: 10.1007/s00431-009-1081-2
- Dominguez J, Gali N, Blanco S, Pedroso P, Prat C, Matas L, et al. Detection of *Streptococcus pneumoniae* antigen by a rapid immunochromatographic assay in urine samples. *Chest* 2001; **119**: 243–9.
- Nambu A, Saito A, Araki T, Ozawa K, Hiejima Y, Akao M, et al. Chlamydia pneumoniae: comparison with findings of *Mycoplasma pneumoniae* and *Streptococcus pneumoniae* at thin-section CT. *Radiology* 2006; **238**: 330–8. doi: 10.1148/radiol.2381040088
- Okada F, Ando Y, Matsushita S, Ishii R, Nakayama T, Morikawa K, et al. Thin-section CT findings of patients with acute *Streptococcus pneumoniae* pneumonia with and without concurrent infection. *Br J Radiol* 2012; **85**: 357–64. doi: 10.1259/bjr/18544730
- Yagihashi K, Kurihara Y, Fujikawa A, Matsuoka S, Nakajima Y. Correlations between computed tomography findings and clinical manifestations of *Streptococcus pneumoniae* pneumonia. *Jpn J Radiol* 2011; **29**: 423–8. doi: 10.1007/s11604-011-0574-x
- Oikonomou A, Müller NL, Nantel S. Radiographic and high-resolution CT findings of influenza virus pneumonia in patients with hematologic malignancies. *AJR Am J Roentgenol* 2003; **181**: 507–11. doi: 10.2214/ajr.181.2.1810507
- Kim EA, Lee KS, Primack SL, Yoon HK, Byun HS, Kim TS, et al. Viral pneumonias in adults: radiologic and pathologic findings. *Radiographics* 2002; **22**: 137–49. doi: 10.1148/radiographics.22.suppl\_1.g02oc15s137
- Tanaka N, Emoto T, Suda H, Kunihiro Y, Matsunaga N, Hasegawa S, et al. High-resolution computed tomography findings of influenza virus pneumonia: a comparative study between seasonal and novel (H1N1) influenza virus pneumonia. *Jpn J Radiol* 2012; **30**: 154–61. doi: 10.1007/s11604-011-0027-6

12. Webb WR, Muller NL, Naidich DP. High-resolution computed tomography findings of lung disease. In: Webb WR, Müller NL, Naidich DP, eds. *High-resolution CT of the lung*. 3rd edn. Philadelphia, PA: Lippincott Williams & Wilkins; 2001. pp. 71–192.
13. Austin JH, Müller NL, Friedman PJ, Hansell DM, Naidich DP, Remy-Jardin M, et al. Glossary of terms for CT of the lungs: recommendations of the Nomenclature Committee of the Fleischner Society. *Radiology* 1996; **200**: 327–31. doi: 10.1148/radiology.200.2.8685321
14. McCullers JA. Insights into the interaction between influenza virus and pneumococcus. *Clin Microbiol Rev* 2006; **19**: 571–82. doi: 10.1128/CMR.00058-05
15. Narayana Moorthy A, Narasaraju T, Rai P, Perumalsamy R, Tan KB, Wang S, et al. In vivo and in vitro studies on the roles of neutrophil extracellular traps during secondary pneumococcal pneumonia after primary pulmonary influenza infection. *Front Immunol* 2013; **4**: 56.
16. Brundage JF. Interactions between influenza and bacterial respiratory pathogens: implications for pandemic preparedness. *Lancet Infect Dis* 2006; **6**: 303–612. doi: 10.1016/S1473-3099(06)70466-2
17. Peltola VT, McCullers JA. Respiratory viruses predisposing to bacterial infections; role of neuraminidase. *Pediatr Infect Dis* 2004; **23**: 87–97.
18. Tashiro M, Ciborowski P, Klenk HD, Pulverer G, Rott R. Role of *Staphylococcus* protease in the development of influenza pneumonia. *Nature* 1987; **325**: 536–7. doi: 10.1038/325536a0
19. Seki M, Yanagihara K, Higashiyama Y, Fukuda Y, Kaneko Y, Ohno H, et al. Immunokinetics in severe pneumonia due to influenza virus and bacteria coinfection in mice. *Eur Respir J* 2004; **24**: 143–9.
20. Shahangian A, Chow EK, Tian X, Kang JR, Ghaffari A, Liu SY, et al. Type 1 IFNs mediate development of post influenza bacterial pneumonia in mice. *J Clin Invest* 2009; **119**: 1910–20.
21. Pitter LA, Hall-Stoodley L, Rutkowski MR, Harmsen AG. Influenza virus infection decreases tracheal mucociliary velocity and clearance of *Streptococcus pneumoniae*. *Am J Respir Cell Mol Biol* 2010; **42**: 450–60.
22. Lourida DB, Blummenfeld HL, Ellis JT, Kilbourne ED, Rogers DE. Studies in the pandemic of 1957-1958: II. Pulmonary complications of influenza. *J Clin Invest* 1959; **38**: 213–65.
23. Lindsay MI, Hermann EC, Morrow GW, Brown AL Jr. Hong Kong influenza: clinical, microbiologic, and pathologic features in 127 cases. *JAMA* 1970; **214**: 1825–32.
24. Oseasohn R, Adelson L, Kaji M. Clinicopathologic study of thirty-three fatal cases of Asian influenza. *N Engl J Med* 1959; **269**: 510–18. doi: 10.1056/NEJM195903122601101
25. Giles C, Shuttleworth EM. Post-mortem findings in 46 influenza deaths. *Lancet* 1957; **2**: 1224–5.
26. Oliveira EC, Marik PE, Colice G. Influenza pneumonia: a descriptive study. *Chest* 2001; **119**: 1717–23.
27. Leung AN, Gosselin MV, Napper CH, Braun SG, Hu WW, Wong RM, et al. Pulmonary infections after bone marrow transplantation: clinical and radiographic findings. *Radiology* 1999; **210**: 699–710. doi: 10.1148/radiology.210.3.r99mr39699
28. Fujita J, Bandoh S, Yamaguchi M, Higa F, Tatayama M. Chest CT findings of influenza virus-associated pneumonia in 12 adult patients. *Influenza Other Respir Viruses* 2007; **1**: 183–7. doi: 10.1111/j.1750-2659.2008.00034.x
29. Ichikado K, Suga M, Gushima Y, Johkoh T, Iyonaga K, Yokoyama T, et al. Hyperoxia-induced diffuse alveolar damage in pigs: correlation between thin-section CT and histopathologic findings. *Radiology* 2000; **216**: 531–8. doi: 10.1148/radiology.216.2.r00j105531
30. Feldman PS, Cohan MA, Hierholzer WJ Jr. Fatal Hong Kong influenza: a clinical, microbiological and pathological analysis of nine cases. *Yale J Biol Med* 1972; **45**: 49–63.
31. Soto PJ Jr, Broun GO, Wyatt JP. Asian influenza pneumonia: a structural and virologic analysis. *Am J Med* 1959; **27**: 18–25.
32. Johkoh T, Itoh H, Müller NL, Ichikado K, Nakamura H, Ikezoe J, et al. Crazy-paving appearance at thin-section CT: spectrum of disease and pathologic findings. *Radiology* 1999; **211**: 155–60. doi: 10.1148/radiology.211.1.r99ap10155
33. Heitzman ER. Pneumonia and lung abscess. In: Heitzman ER, ed. *The lung. Radiologic-pathologic correlations*. 2nd edn. St Louis, MO: Mosby; 1984. pp. 194–234.
34. Spencer H. The bacterial pneumonias. In: Spencer H, ed. *Pathology of the lung*. 4th edn. Oxford, UK: Pergamon Press; 1985. pp. 167–212.